Comparison of the activating effect of dimethyl ether and propene on the homogeneous partial oxidation of methane

Fikri Sen, Tina Kasper*,Stefan Haferkamp, Anton Ditmann, Ulf Bergmann, Burak Atakan

Thermodynamics, IVG, University of Duisburg-Essen, Lotharstr. 1, 47057 Duisburg, Germany

Abstract

The homogeneous partial oxidation of methane (CH_4) can provide a pathway towards production of target chemicals and synthesis gas with small exergy losses. The thermal conversion of methane is studied in fuel-rich mixtures at high pressures (6 bar) in a tubular reactor at relatively long reaction times (>1 s). The variation of the gas composition at the reactor outlet is determined by time-of-flight mass spectrometry. Experimental concentration profiles as a function of temperature indicate the temperature required to instigate a reaction. They are compared to simulations and serve as validation data for reaction mechanism development for these unusual reaction conditions. The low reactivity of neat methane can be overcome by the addition of additives and the activating effect propene and dimethyl ether (CH_3OCH_3) has been investigated.

Introduction

Engines typically convert the chemical energy in a fuel to heat and mechanical energy. However, it is conceivable that under appropriate conditions a fraction of the fuel is only oxidized partially at the cost of smaller heat release and mechanical energy transfer. Some partially oxidized substances are useful chemicals, e.g. syngas ($CO + H_2$), formaldehyde (CH_2O) and methanol (CH_3OH).

Under fuel-rich conditions soot can form in engines fueled by methane [1] showing that C-C-coupling and condensation reactions as well as hydrogenation and dehydrogenation reactions are possible within an engine. While soot, polyaromatic hydrocarbons and unburnt hydrocarbons are usually undesired emissions [2], they can also be considered an untapped reservoir of chemical energy. Following this line of thought, the motor could be considered a multifunctional tool that enables the conversion of the available energy in the fuel to alternatively mechanical energy, heat, and useful chemicals.

From the point of view of minimizing the loss of available energy (exergy) a production of chemicals by partial oxidation in a power generation process can be beneficial [3]. For example, the existing commercial process for the production of methanol from natural gas involves the intermediate formation of syngas which is then converted into methanol by a catalytic process [4]. The two-step process and the highly endothermic reforming reaction lead to significant losses of available energy compared to direct conversion of methane to methanol, where the oxidation process is intercepted at the stage of initial oxidation. The same is true for the production of formaldehyde from methanol by an additional catalytic oxidation step [5]. The kinetic fundamentals of the homogeneous partial oxidation of methane to methanol have been studied extensively in recent years by Glarborg et al. in high-pressure flow reactors [6, 7, 8, 9, 10]. In addition, Rytz et al. could show that the methane conversion decreases when a high selectivity for methanol is realized [11].

Natural gas is a clean-burning and abundant energy resource, but for transport it needs to be liquefied at high costs or converted to hydrocarbon liquids using for example expensive Fischer-Tropsch technology. Consequently in recent years there has been a renewed interest in processes for acetylene (C_2H_2) and ethylene (C_2H_4) production from natural gas, in particular as the first step in gas-to-liquid processes [12, 13]. Combined acetylene and hydrogen production has been demonstrated in a partial oxidation and a pyrolysis mode at the pilot plant stage [12]. The complex reactions underlying the conversion were not investigated. However, a detailed understanding of the chemical processes involved in C-C coupling reactions can help to avoid unfavorable reaction conditions, e.g. because of soot formation.

Neat methane shows only low reactivity as indicated by a need for high conversion temperatures. The addition of additives or co-reactants can reduce the temperatures required to start the conversion [10] and the activating effect of propene and dimethyl ether has been investigated here. Dimethyl ether has been shown to promote the ignition of methane in HCCI engines [14] and is therefore of particular interest in the frame work of multifunctional conversion processes at high pressure.

Specific Objectives

The reactions underlying multifunctional chemical and energy conversion processes are investigated experimentally using a flow reactor in this work. The experiments target the partial oxidation of methane and dimethyl ether. One of the aims of the study is to identify reasonable target chemicals. The partial oxidations are studied under fuel-rich conditions ($\phi = 20$) at high pressures (6 bar) and high temperatures

* Corresponding author: tina.kasper@uni-due.de

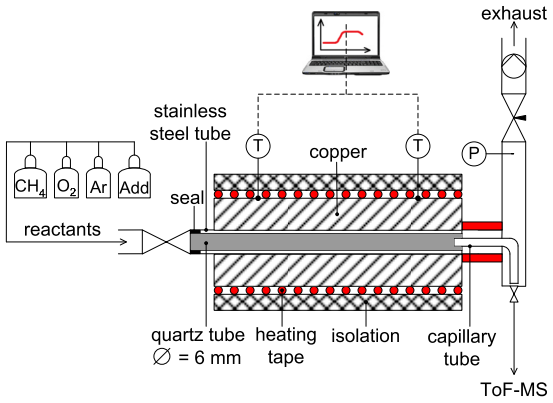

Fig. 1: Schematic diagram of the set-up

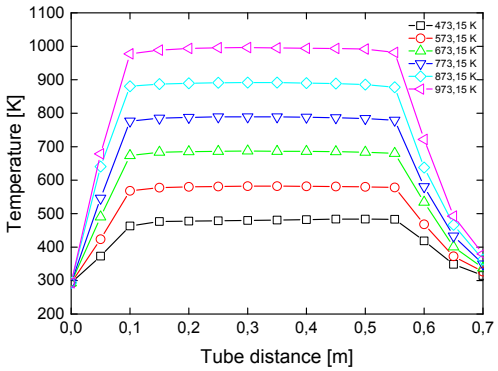

Fig. 2: Measured temperature profiles along the reactor tube with a reaction zone of 45 cm for the labeled nominal temperatures.

(T_{max} = 1030 K) for long residence times in a tubular reactor. The gas composition at the reactor outlet is determined by time-of-flight mass spectrometry (ToF-MS). Through variation of reactor temperature an overview of the maximum mole fractions of target chemicals, the temperature of observed reaction onset and the optimal temperature to increase target yields can be determined.

The experimental results are compared to kinetic simulations to assess how well the flow reactor data are reproduced for these uncommon reaction conditions. Deviations between experiment and simulations indicate the ability to simulate the absolute mole fractions, correct reaction onset temperatures and the relative changes of composition with temperature.

Experimental Setup

Experimental setup

The experimental setup used in the experiments reported here is shown in Fig. 1. The experiments were carried out in a quartz flow reactor with an inner diameter of 6 mm. The overall reactor length is 70 cm. Because the experiments are conducted at pressures above atmosphere, the quartz tube is fitted into a stainless steel tube for safety reasons. When the reactor is at room temperature there is only a minimal gap between quartz and steel; at higher temperatures the gap increases. The gap is sealed in the front of the reactor. At the end of the quartz reactor a small part of the process gases may diffuse into the gap. In this way it is ensured that the pressure gradient between process pressure and outside pressure is not across the quartz tube but across the steel tube. The tube assembly is enclosed in a round copper shell with a thickness of 11.5 cm. The copper shell leads to a homogeneous temperature distribution in the quartz reactor when the whole assembly is heated externally by heating tape. The temperature profiles measured with a thermocouple on the centerline of the quartz tube for different set temperatures of the heating tape are shown in Fig. 2. The homogeneously heated length of the reactor (the reaction zone) is 45 cm. The reactor ends in a KF40-T piece. It connects the reactor to a pressure regulation valve and a vacuum pump on one side and to a fine metering valve (Pfeiffer Vacuum) as inlet to a time-of-flight mass spectrometer on the other side. To minimize recirculation and contact time to the stainless steel in the KF piece before the mass spectrometric composition analysis, the process gases pass through a capillary at the outlet of the quartz reactor which ends directly in front of the fine metering valve.

For the analysis of the process gas, the fine metering valve is adjusted so that the pressure in the ionization chamber of the mass spectrometer is the same ($3 \cdot 10^{-7}$ mbar) for all measurements. The gas sample is ionized by electron ionization. The kinetic energy of the electrons is 20 eV. Mass spectra are recorded with a repetition rate of 20 kHz. The ions are registered by a multichannel plate. Its output voltage is amplified and digitized by a FAST card (FAST P7887) with 10^5 channels of 0.25 ns width. The FAST card is operated in ion counting mode (TDC-mode). A mass resolution of $m/\Delta m \approx 2000$ can be realized in these experiments. The resulting relative signals are quantified by comparison to relative signals from calibration measurements. For these measurements binary cold gas mixtures of known composition are passed through the reactor and analyzed with the same instrument settings as the chemical conversion measurements. According to equation 1 a calibration factor k can be determined and used, also in conjunction with equation 1, to calculate mole fractions in mixtures of unknown composition.

$$\frac{S_i}{S_{Ar}} = \frac{x_i}{x_{Ar}} \cdot k_i \qquad (1)$$

$S_{i/Ar}$: integrated signal intensity of species i or argon
$x_{i/Ar}$: the mole fraction of species i or argon
k_i: calibration factor of species i

Argon serves as reference because it is used in large excess as dilution gas in all experiments and its mole fraction is almost constant even if reactions occur in the gas mixture. The high dilution of the reacting gas mixture also ensures a nearly isothermal reaction,

Table 1: Reaction conditions

Experiment/ Simulation	CH_4	O_2	C_3H_6	DME	Ar	p	T	ϕ	τ
			[Mol%]			[bar]	[K]	[-]	[s]
A	35.7	3.57	1.07	-	59.6	6	633-1030	21.35	7.6-12.3
B	35.7	3.57	1.79	-	58.9	6	633-1030	22.25	7.6-12.3
C	35.7	3.57	-	1.07	59.6	6	531-993	20.90	4.5-9.2
D	35.7	3.57	-	1.79	58.9	6	531-993	21.50	4.5-9.2

independent of energy release by the conversion reactions.

As a consistency check element balances for C, H and O were calculated. The mole fractions of methane, oxygen, argon, water, hydrogen and carbon monoxide can be inferred from those balances and are reported here instead of the results obtained by direct calibration because their absolute errors are estimated to be smaller. When direct calibration factors are used the uncertainties of two independent measurements are added while a calibration factor derived from an element balance is only affected by the uncertainties of the chemical conversion experiment. The uncertainties are estimated to be on the order of 30% for the species calibrated by element balances and on the order of a factor of 2 for methanol and formaldehyde calibrated by direct calibration.

Reaction conditions

The experiments were performed at 6 bar, 531-1030 K (increased in 50 K steps) and with a stoichiometric ratio of ϕ = 20.9-22.25. The stoichiometric ratios ϕ are based on the reaction equations (2)-(4). Table 1 summarizes the reaction conditions. τ is the residence time in the reaction zone.

$$CH_4 + 2O_2 \longrightarrow CO_2 + 2H_2O \quad (2)$$

$$C_3H_6 + 4.5O_2 \longrightarrow 3CO_2 + 3H_2O \quad (3)$$

$$CH_3OCH_3 + 3O_2 \longrightarrow 2CO_2 + 3H_2O \quad (4)$$

Modeling study

The experiment is simulated using the program Cantera in a Python environment [15]. The reactor was divided into a network of smaller units and the subroutine "Cantera.reactor" used to solve the time dependent conservation equations of this series of perfectly homogeneous reactors. The gas feed to the first reactor has the initial gas composition. The composition change during the residence time in this part of the reactor at the measured reactor temperature is simulated. Then the gas passes into the next reactor and so on. The gas-inlet of the reactor *n* is the gas-outlet of reactor *n-1*.

This simulation strategy is only applicable if the reactor is operated under plug-flow condition for which neither radial not axial diffusion lead to significant dispersion of the gases. The dispersion factors have been calculated following the procedure employed by Glarborg et al. and have the same magnitude as in their experiments [9]. They are show in Fig. 3. At flow rates of 280 sccm and Bodenstein numbers of approximately Bo = 20-34 dimensionless dispersions of D = 0.15-0.21 for our experiment were calculated. The conditions are thus close to optimal plug-flow conditions.

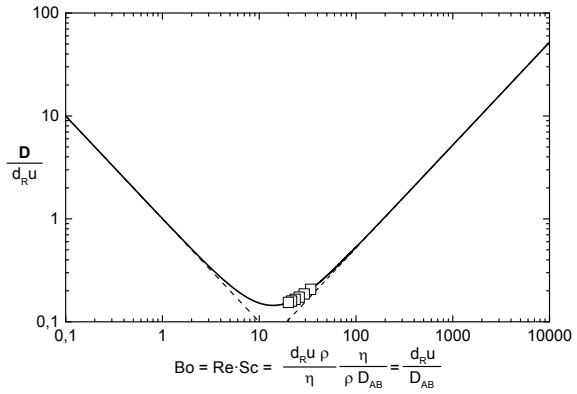

Fig. 3: Axial dispersion ($D/d_R\,u$) for streamline flow in the reactor tube.

For the simulations the chemical kinetic mechanisms of Curran et al. [16] have been used. It has been developed and tested for other reaction conditions [16] and include the fuel (methane) and additives (propene and dimethyl ether) of interest in this study.

Results and Discussion

Fig. 4 show the mole fraction profiles of methane conversions under fuel-rich conditions activated by propene and dimethyl ether, respectively. Experimental results (dotted lines) are compared to simulation results of the experiment (solid lines). The measurements with propene additive have been reported before [17] and are provided here for comparison. They have been obtained with an older version of the experimental setup and were quantified using only direct calibration. The main changes to the flow reactor have been a shortening of the total reactor length resulting in shorter residence times and the addition of the copper shell to implement more homogeneous heating. In particular the use of element balances in the quantification procedure has improved the agreement between simulation and experiment for the dimethyl ether experiments compared to the propene experiments for the product

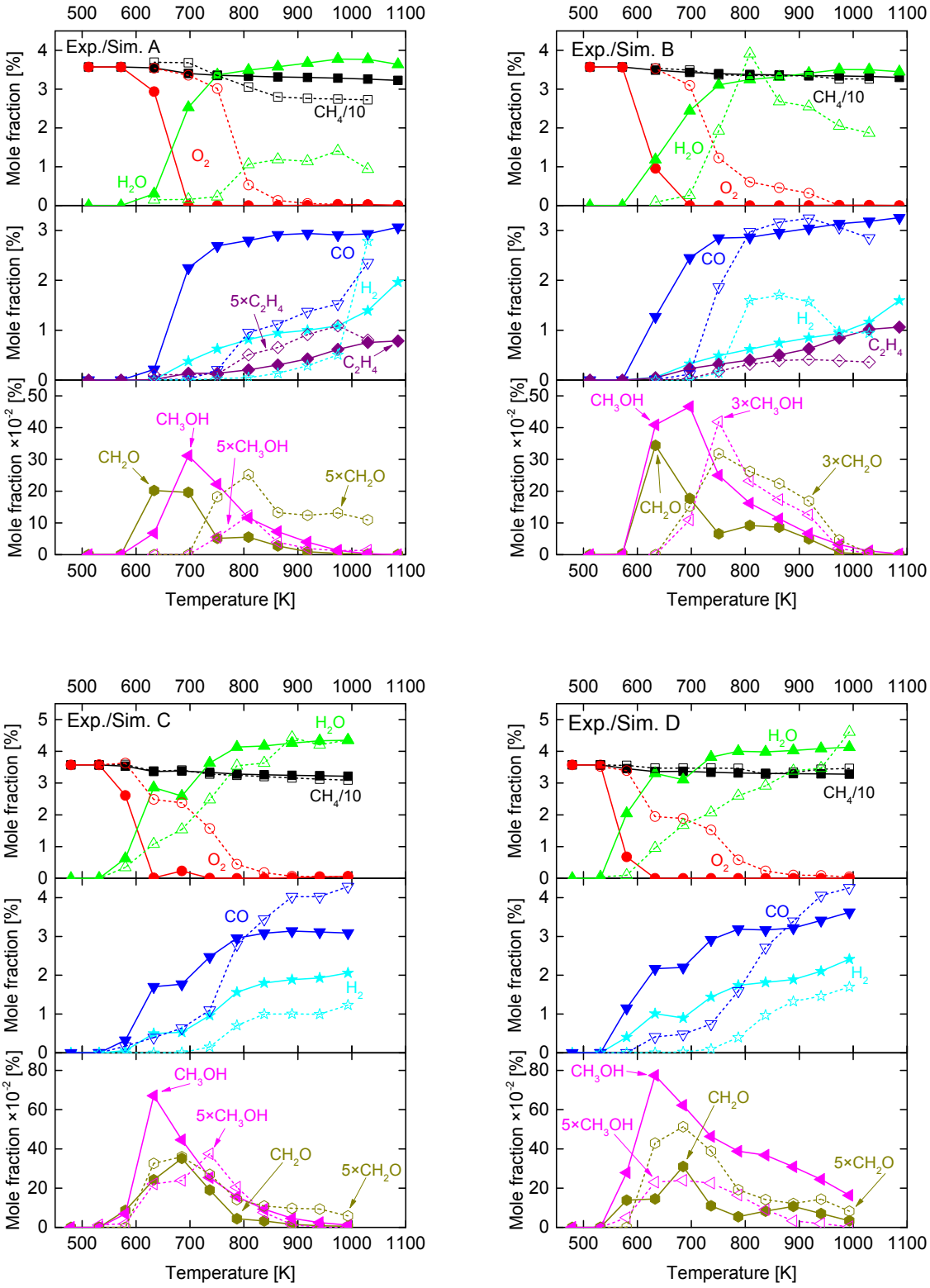

Fig. 4: Results of experiments (dotted lines) and simulations (solid lines) with mechanism of Metcalfe et al. [16] A-D as function of the reactor temperature at 6 bar and ϕ = 20.90-22.25. Top left : Experiment and simulation A (3 sccm C_3H_6), Top right: Experiment and simulation B (5 sccm C_3H_6), Bottom left: Experiment and simulation C (3 sccm DME), Bottom right: Experiment and simulation D (5 sccm DME).

species water, hydrogen and carbon monoxide. For the partially oxidized products methanol and formaldehyde the deviation between simulation and experiment is close to a factor of 5. This factor is outside our estimated uncertainty for the mole fractions of these species and indicates that while the calibration procedure for these species needs to be refined further also the predictions of the chemical mechanisms are likely not accurate.

In propene experiments (A and B) ethene could be identified and quantified as product species. Its mole fraction is about 0.22% in experiment A and 0.41% in experiment B. The mole fraction in experiment A is comparable to the mole fraction of ethene formed in the thermal conversion of neat methane [17]. The addition of dimethyl ether seems to suppress the formation of C-C bonds.

For both fuels, the general trends of the temperature dependent composition curves are captured correctly. The temperature of the reaction onset is shifted by approximately 100 K for experiments A and B with propene additive and 50 K for experiments C and D with dimethyl ether additive. Compared to neat methane experiments [17], both additives lower the initiation temperature. The profile shapes of the temperature dependent mole fraction profiles are reproduced slightly better for the experiment with propene.

The comparison of the experimental and the simulated water, carbon monoxide and hydrogen profiles reveals a steeper mole fraction increase with temperature in the simulation than in the experiment for experiments C and D with dimethyl ether additive. This observation indicates that once the conversion process has started the gases react too fast in the simulation. With increasing dimethyl ether fraction in the initial gas mixture this effect becomes more pronounced as can be seen from the comparison of experiment C and D.

Conclusions

The present study investigates the homogeneous partial oxidation of methane after activation of the reaction with propene and dimethyl ether. The experiments are conducted in a flow reactor at 6 bar, 531-1030 K and fuel rich stoichiometries of ϕ = 20.9-22.25. Both additives active the reaction and lower the reaction temperatures. Dimethyl ether is more effective than propene and lowers the temperature of reaction onset by an additional 50 K. The product composition is only slightly influenced by the choice of additive. Most notably, the ethene mole fractions are below the detection limit in the dimethyl ether experiments but reach the lower percent level in the experiments with propene.

The experimental results are compared with modeling results using an elementary reaction mechanisms by Curran et al.. Improvements to the calibration procedure in the experiments with dimethyl ether lead to much better quantitative agreement between simulation and experiment for the main species carbon monoxide, water and hydrogen. For products that are only formed with low concentrations such as methanol and formaldehyde the deviations between measured and simulated mole fractions are larger than the experimental uncertainty. This observation emphasizes the need for better chemical models and accurate validation data to progress model based planning of thermochemical conversion reactions and to develop the ability to predict target chemical yields.

Acknowledgements

The authors would like to thank Mr. Andreas Görnt, Mr. Stephan Steinbrink and Mr. Erdal Akyildiz for their technical support. Financial support of this work (KA3871_1_1) by the Deutsche Forschungsgemeinschaft within the framework of the DFG research unit FOR 1993 'Multi-functional conversion of chemical species and energy' is gratefully acknowledged.

References

[1] D. S. Bullock, J. S. Olfert, Size, volatility, and effective density of particulate emissions from a homogeneous charge compression ignition engine using compressed natural gas, Journal of Aerosol Science 75 (2014) 1–8. http://dx.doi.org/10.1016/j.jaerosci.2014.04.005 doi:10.1016/j.jaerosci.2014.04.005.

[2] T. J. Jacobs, D. N. Assanis, The attainment of premixed compression ignition low-temperature combustion in a compression ignition direct injection engine, Proceedings of the Combustion Institute 31 (2007) 2913–2920. http://dx.doi.org/10.1016/j.proci.2006.08.113 doi:10.1016/j.proci.2006.08.113.

[3] B. Atakan, Gas turbines for polygeneration? a thermodynamic investigation of a fuel rich gas turbine cycle., International Journal of Thermodynamics 14 (4) (2011) 185–192.

[4] H. D. Gesser, N. R. Hunter, C. B. Prakash, The direct conversion of methane to methanol by controlled oxidation, Chemical Reviews 85 (4) (1985) 235–244. http://dx.doi.org/10.1021/cr00068a001 doi:10.1021/cr00068a001.

[5] G. Reuss, W. Disteldorf, A. O. Walter, A. Hilt, Ullmann's Encyclopedia of Industrial Chemistry: Formaldehyde, Vol. 15, Wiley-VCH Verlag GmbH and Co. KGaA, Weinheim, 2012.

[6] S. Gersen, A. V. Mokhov, J. H. Darmeveil, H. B. Levinsky, P. Glarborg, Ignition-promoting effect of no2 on methane, ethane and methane/ethane mixtures in a rapid compression machine, Proceedings of the Combustion Institute 33 (2011) 433–440. http://dx.doi.org/10.1016/j.proci.2010.05.097 doi:10.1016/j.proci.2010.05.097.

[7] P. Glarborg, L. L. B. Bentzen, Chemical effects of a high co2 concentration in oxy-fuel combustion of methane, Energy & Fuels 22 (1) (2008) 291–296. http://dx.doi.org/10.1021/-ef7005854 doi:10.1021/ef7005854.

[8] C. L. Rasmussen, P. Glarborg, Direct partial oxidation of natural gas to liquid chemicals: Chemical kinetic modeling and global optimization, Industrial and Engineering Chemistry Research 47 (17) (2008) 6579–6588. http://dx.doi.org/10.1021/ie800137d doi:10.1021/ie800137d.

[9] C. L. Rasmussen, J. Hansen, P. Marshall, P. Glarborg, Experimental measurements and kinetic modeling of co/h-2/o-2/no, conversion at high pressure, International Journal of Chemical Kinetics 40 (8) (2008) 454–480. http://dx.doi.org/10.1002/kin.20327 doi:10.1002/kin.20327.

[10] C. L. Rasmussen, A. E. Rasmussen, P. Glarborg, Sensitizing effects of no(x) on ch(4) oxidation at high pressure, Combustion and Flame 154 (3) (2008) 529–545. http://dx.doi.org/10.1016/j.combustflame.2008.01.012 doi:10.1016/j.combustflame.2008.01.012.

[11] D. Rytz, A. Baiker, Partial oxidation of methane to methanol in a flow reactor at elevated pressure, Industrial and Engineering Chemistry Research 30 (10) (1991) 2287–2292. http://dx.doi.org/10.1021/ie00058a007 doi:10.1021/ie00058a007.

[12] K. R. Hall, A new gas to liquids (gtl) or gas to ethylene (gte) technology, Catalysis Today 106 (1-4) (2005) Technol Inst, KVIV. http://dx.doi.org/10.1016/j.cattod.2005.07.176 doi:10.1016/j.cattod.2005.07.176.

[13] O. A. Rokstad, O. A. Lindvaag, A. Holmen, Acetylene pyrolysis in tubular reactor, International Journal of Chemical Kinetics 46 (2) (2014) 104–115. http://dx.doi.org/-10.1002/kin.20830 doi:10.1002/kin.20830.

[14] S. Sato, D. Yamashita, N. Lida, Influence of the fuel compositions on the homogeneous charge compression ignition combustion, International Journal of Engine Research 9 (2) (2008) 123–148. http://dx.doi.org/10.1243/-14680874JER02607 doi:10.1243/14680874JER02607.

[15] D. G. Goodwin, An open-source, extensible software suite for cvd process simulation, in: F. M. M. Allendorf, F. Teyssandier (Eds.), Chemical Vapor Deposition XVI and EUROCVD 14, ECS Proceedings Volume 2003-08, The Electrochemical Society, 2003, pp. 155–162.

[16] W. K. Metcalfe, S. M. Burke, S. S. Ahmed, H. J. Curran, A hierarchical and comparative kinetic modeling study of c-1 - c-2 hydrocarbon and oxygenated fuels, International Journal of Chemical Kinetics 45 (10) (2013) 638–675. http://dx.doi.org/-10.1002/kin.20802 doi:10.1002/kin.20802.

[17] F. Sen, T. Kasper, U. Bergmann, R. Hegner, B. Atalan, Partial oxidation of methane at elevated pressures and effects of propene and ethane as additive: experiment and simulation, Zeitschrift für Physikalische Chemie (2015) in press2015.